How Much Is Enough? Optimal Support Payments in a Renewable-Rich Power System

Tuomas Rintamäki[a], Afzal S. Siddiqui[b,c,*], Ahti Salo[a]

[a]*Systems Analysis Laboratory, Department of Mathematics and Systems Analysis, School of Science, Aalto University, Finland*

[b]*Department of Statistical Science, University College London, United Kingdom*

[c]*Department of Computer and Systems Sciences, Stockholm University, Sweden*

Abstract

The large-scale deployment of intermittent renewable energy sources may cause substantial power imbalance. Together with the transmission grid congestion caused by the remoteness of these sources from load centers, this creates a need for fast-adjusting conventional capacity such as gas-fired plants. However, these plants have become unprofitable because of lower power prices due to the zero marginal costs of renewables. Consequently, policymakers are proposing new measures for mitigating balancing costs and securing supply. In this paper, we take the perspective of the regulator to assess the effectiveness of support payments to flexible generators. Using data on the German power system, we implement a bi-level programming model, which shows that such payments for gas-fired plants in southern Germany reduce balancing costs and can be used as part of policy to integrate renewable energy.

Keywords: Renewable energy, Support payments, Day-ahead market, Balancing market, Congestion management, Mathematical programming with equilibrium constraints

---

*Corresponding author. Tel.: +44 20 7679 1871
Email addresses: `tuomas.rintamaki@aalto.fi` (Tuomas Rintamäki), `afzal.siddiqui@ucl.ac.uk` (Afzal S. Siddiqui), `ahti.salo@aalto.fi` (Ahti Salo)

1. Introduction

In deregulated electricity industries, the expansion of wind and solar power has decreased power prices and, thus, eroded the viability of coal, lignite, and gas-fired conventional electricity generation units (Winkler et al., 2016). At the same time, the intermittency of renewables and insufficient transmission capacity has increased the need for grid congestion management and flexible conventional generation capacity (Van den Bergh et al., 2015). Indeed, the lack of flexibility may risk grid stability under scenarios with high load or sudden changes in renewable energy generation.

As a potential solution to the threat to security of supply in the long term, capacity markets to entice conventional power plants have been proposed. In these schemes, an authority ensures a sufficient level of capacity through payments or obligations (Hary et al., 2016). On the other hand, German Federal Ministry for Economic Affairs and Energy (BMWi) (2014) envisages an energy-only "electricity market 2.0" scheme that permits high price peaks, develops intraday markets, and promotes new technologies such as demand response, for instance.

As a response to insufficent flexible generation capacity in southern Germany, a regional transmission system operator (TSO), TenneT, and the Federal Network Agency, Bundesnetzagentur, have agreed to compensate fixed costs of two flexible plants via support payments (TenneT TSO GmbH, 2013). Therefore, in this paper, we develop a complementarity model to assess the increased dispatch of fast-adjusting conventional capacity through support payments, which, in effect, reduce the bid prices of these generators. Specifically, we cast the sequential model in Kunz (2013) as a bi-level problem in which the day-ahead decisions are taken at the upper level and congestion management decisions at the lower level. The latter are guided by the upper-level support payment decisions that the regulator takes in order to minimize the total generation costs. We develop a novel set of constraints to enforce the merit order and cast the problem as a mixed-integer linear program (MILP) by using a linearization technique (Gabriel and Leuthold, 2010). Hence, we assess the performance of a recently implemented regulation for a realistic test network via a rigorous mathematical programming approach.

We calibrate the model to the German power system using realistic data and identify the congested parts of the transmission network to provide insights about the geographical distribution of optimal support payments under different demand and renewable energy scenarios. We also test the performance of the optimal decisions by introducing spatially correlated imbalances in the balancing market. Moreover, we contribute to the ongoing debate by comparing the optimal support payments to the nodal pricing mechanism (Leuthold et al., 2008) and demonstrate that they lead to similar patterns of generation that reduce re-dispatching. In particular, we find that re-dispatch volumes are halved when support payments are introduced. We also extend the model to multiple time periods to show how support payments mitigate the intermittency of renewables by utilizing the fast-ramping capabilities of the flexible units. Thus, alternative market designs such as support payments and nodal pricing improve the flexibility of the power system and reduce the costs of integrating renewables.

The paper is organized as follows. In Section 2, we discuss complementarity models of electricity markets, the challenges posed by the higher penetration of renewables in the day-ahead and balancing markets, and the relevant policy alternatives. Section 3 presents the structure of our bi-level model, and Section 4 gives numerical results for a model calibrated to the German power system along with sensitivity analysis of the optimal decisions. We provide conclusions on the likely impacts of support payments in Germany and discuss directions for future research in Section 5.

2. Literature review

Complementarity models are often used to analyze electricity markets in which prices are formed endogenously and strategic interactions occur among players. Ruiz et al. (2013) give an overview of these models, and a thorough treatise can be found in Gabriel et al. (2013). Leuthold et al. (2012) develop a large-scale perfect competition model of the European electricity market that covers transmission, variable demand, wind power, and pumped storage, for example. In bi-level models, a group of players in the lead role make optimal decisions anticipating the reaction of a group of follower players, e.g., see Baringo and Conejo (2011).

Kunz (2013) presents a sequential model for Germany with a high level of wind generation in which the production schedules determined by a day-ahead market model ignoring the physical transmission network are fed into a congestion management model, which minimizes the re-dispatch costs, i.e., the costs of relieving congestion. Kunz (2013) uses data on realistic projections to 2020 of the increase in demand and renewable energy generation in Germany and finds that annual national congestion management costs increase from €40 million to €147 million without transmission grid extensions.

The need for fast-ramping units to balance generation from intermittent renewables is supported by recent empirical data, e.g., Rintamäki et al. (2014) show that the variability of wind and solar power increases the volatility of German hourly and daily electricity prices. Huber et al. (2014) conclude that there is a dramatic increase in flexibility requirements when the share of renewables of annual electricity consumption exceeds 30%. However, renewable generation has a negative impact on power prices due to its zero marginal costs and prevents the deployment of high-cost flexible plants (Würzburg et al., 2013).

Also, Ueckerdt et al. (2015) show that gas-fired plants are required when short-term variability of renewables is introduced into a long-term German power system model with an 80% emission reduction target. Indeed, gas-fired plants have lower CO_2 emissions and higher fuel efficiency than coal plants (Gutiérrez-Martín et al., 2013). However, major utilities in the UK, France, Germany, and Italy, among others, have recently closed or mothballed gas-fired power plants in response to low profitability (Caldecott and McDaniels, 2014).

Apart from flexible gas-fired plants, there are several other mechanisms to integrate renewables into power systems. At specific sites, the variability of wind power can be reduced by coupling it with wave power (Fusco et al., 2010). Weigt et al. (2010) analyze the economic viability of high-voltage direct current (HVDC) transmission lines from windy northern Germany to load centers in the west and south assumping extensive wind power deployment. They conclude that the welfare gains resulting from full wind power utilization and lower price levels would quickly cover the lines' investment costs. In a similar vein, Jaehnert et al. (2013) postulate that the expansion of the cross-border HDVC network allows the hydro-dominant power systems in the Nordic countries to balance the variability of renewable generation in continental Europe by adjusting hydro production. On the demand side, more flexible pricing schemes could also integrate renewables (Dupont et al., 2014). Likewise, storage and power-to-gas technologies have been explored to increase flexibility (Jentsch et al., 2014; Schill and Kemfert, 2011).

Price-based policies, which directly grant the generating capacity a payment, have been implemented in Spain and Italy, for example (Batlle et al., 2007). In Italy, in particular, the policy aimed to keeping existing capacity in operation and compensates generators when prices are too low (Benini et al., 2006). Conversely, quantity-based policies, e.g., as implemented in the UK, determine the capacity payment in an auction to cover a quantity considered to secure supply. Typically, they enforce the availability of the procured capacity by setting a strike price for the spot market price above which the generators need to compensate the regulator (Vazquez et al., 2002). Hach and Spinler (2016) show that capacity payments can reduce the impact of renewable energy generation on the profitability of gas-fired plants and, thus, prevent their mothballing.

By contrast, energy-only policies such as the "electricity market 2.0" concept have the virtue that they minimize interventions in the electricity market. Even under these policies, some kind of back-up reserves are maintained (Batlle and Rodilla, 2010). A BMWi white paper (Bundesministerium für Wirtschaft und Energie (BMWi), 2015) outlines a reserve capacity based mainly on old lignite plants, which are started up when a market price cannot be formed. Moreover, the white paper describes a reserve to relieve congestion in southern Germany.

Conceptually, our model resembles Morales et al. (2014) and Khazaei et al. (2014) in using a bi-level approach for integrating renewables by comparing alternative market-clearing schemes. However, we seek to find the optimal trade-off between the least-cost day-ahead market dispatch and the support payments, which have the potential to reduce congestion management and balancing costs by enticing the dispatch of flexible but more expensive power plants.

3. Mathematical formulation

3.1. Notation

Sets and indices

Φ	auxiliary decision variables
Ω^{DV}	lower-level dual variables
Ω^{UL}	upper-level primal decision variables
Ω^{LL}	lower-level primal decision variables
$n,k \in N$	nodes
$n' \in N$	reference node
$u,o \in U$	generation types
$t \in T$	time periods
$i \in I$	discrete support payment levels
$\ell \in L$	transmission lines

Parameters

$cons_{n,t}$	consumption at node n during period t
$\bar{s}_{n,u,i}$	support payments levels for unit u at node n
$c^{m}_{n,u}$	bid price of generation of unit u at node n
$c^{up}_{n,u}$	up-reserve bid price of unit u at node n
$c^{down}_{n,u}$	down-reserve bid price of unit u at node n
$g^{max}_{n,u,t}$	maximum generation capacity of unit u at node n during period t
$\varepsilon^{da^{up}}_{n,u}$	day-ahead ramp-up rate of unit u at node n
$\varepsilon^{da^{down}}_{n,u}$	day-ahead ramp-down rate of unit u at node n
$\varepsilon^{reserve^{up}}_{n,u}$	up-reserve deployment rate of unit u at node n
$\varepsilon^{reserve^{down}}_{n,u}$	down-reserve deployment rate of unit u at node n
cap^{max}_{ℓ}	thermal capacity of power line ℓ
$H_{\ell,k}$	branch susceptance matrix $\ell \times k$
$B_{n,k}$	node susceptance matrix $n \times k$
sw_n	reference node switch variable

Scalars

eps	a small positive constant
M_1	a large positive constant
$K_1,...,K_8$	constants for disjunctive constraints
$K_{g^{da}},K_v$	constants for linearization

Variables

$\lambda^{cm}_{n,t}$	re-dispatch price at node n during period t
$\delta_{n,t}$	phase angle at node n during period t
$\gamma_{n,t}$	dual for the swing bus constraint at node n during period t

Positive variables

$s_{n,u}$	support payment for unit u at node n
$g^{f}_{n,u,t}$	full generation of unit u at node n during period t in the day-ahead market
$g^{r}_{n,u,t}$	residual generation of unit u at node n during period t in the day-ahead market
$g^{da}_{n,u,t}$	total day-ahead generation of unit u at node n during period t
$g^{up}_{n,u,t}$	up-reserve deployment of unit u at node n during period t
$g^{down}_{n,u,t}$	down-reserve deployment of unit u at node n during period t
$\beta^{da}_{n,u,t}$	dual for maximum generation capacity of unit u at node n during period t in the day-ahead market
$\beta^{up}_{n,u,t}$	dual for absolute maximum up-reserve deployment of unit u at node n during period t
$\beta^{down}_{n,u,t}$	dual for absolute maximum down-reserve deployment of unit u at node n during period t
$\theta^{up}_{n,u,t}$	dual for relative maximum up-reserve deployment of unit u at node n during period t
$\theta^{down}_{n,u,t}$	dual for relative maximum down-reserve deployment of unit u at node n during period t
$\overline{\mu_{\ell,t}}$	dual for positive line capacity constraint on line ℓ during t
$\underline{\mu_{\ell,t}}$	dual for negative line capacity constraint on line ℓ during t
$v_{n,u,i,t}$	discretization of $s_{n,u} \cdot g^{da}_{n,u,t}$ of unit u at node n during t

Binary variables

$r1,...,r8$	disjunctive variables
$q^{g^{da}}_{n,u,t}$	indicator variables equal to 1 when $g^{da}_{n,u,t} > 0$
$q_{n,u,i}$	indicator variables equal to 1 if i^{th} support payment level is selected
$q^{v}_{n,u,i,t}$	indicator variables equal to 1 when $q^{g^{da}}_{n,u,t}$ and $q_{n,u,i}$ are 1
$f_{n,u,t}$	indicator variables equal to 1 when unit u is fully dispatched
$r_{n,u,t}$	indicator variables equal to 1 when unit u is partially dispatched

3.2. Bi-level formulation

In the upper level of our bi-level model, the objective function of a regulator (1) is to minimize the costs of day-ahead generation, including the possible support payments and the anticipated costs of re-dispatch and real-time balancing power, i.e., increasing (deploying up-reserves) and decreasing (deploying down-reserves) the generation of power plants. In the day-ahead market, supply and demand match at every time period (2) and the generation of plant (n,u) in time period t is the sum of full generation $g^{f}_{n,u,t}$ and residual generation $g^{r}_{n,u,t}$ (3). As per the rules of the German market, physical transmission constraints are neglected at the time of day-ahead dispatch and applied only in the re-dispatching phase. If the decision variable $f_{n,u,t}$ equals to 1, then constraint (4) forces the plant to produce at its maximum capacity. Otherwise, the plant is not fully dispatched. However, if the decision variable $r_{n,u,t}$ in (5) equals to 1, then the plant is operating at a level below its maximum capacity that is set by the decision variable $g^{r}_{n,u,t}$. Constraint (6) ensures that the plant cannot be fully and partially dispatched at the same time. Finally, the inequalities (7) and (8) exclude unrealistic ramping of power plants and avoid discontinuities between time periods.

$$\underset{\Omega^{UL}}{\text{Minimize}} \sum_{t}\sum_{n}\sum_{u}\Big(\left(c^{m}_{n,u}+s_{n,u}\right)g^{da}_{n,u,t}+c^{up}_{n,u}g^{up}_{n,u,t}-c^{down}_{n,u}\,g^{down}_{n,u,t}\Big) \tag{1}$$

s.t.

$$\sum_{n} cons_{n,t} = \sum_{n}\sum_{u} g^{da}_{n,u,t} \qquad \forall t \tag{2}$$

$$g^{da}_{n,u,t} = g^{f}_{n,u,t} + g^{r}_{n,u,t} \qquad \forall n,u,t \tag{3}$$

$$g^{f}_{n,u,t} = f_{n,u,t}\, g^{max}_{n,u,t} \qquad \forall n,u,t \tag{4}$$

$$g^{r}_{n,u,t} \leq r_{n,u,t}\,(g^{max}_{n,u,t} - eps) \qquad \forall n,u,t \tag{5}$$

$$f_{n,u,t} + r_{n,u,t} \leq 1 \qquad \forall n,u,t \tag{6}$$

$$g^{da}_{n,u,t} - (g^{da}_{n,u,t-1} + g^{up}_{n,u,t-1}) \leq \varepsilon^{da^{up}}_{n,u}\, g^{max}_{n,u,t} \qquad \forall n,u, \text{ and } \forall t \geq 2 \tag{7}$$

$$(g^{da}_{n,u,t-1} - g^{down}_{n,u,t-1}) - g^{da}_{n,u,t} \leq \varepsilon^{da^{down}}_{n,u}\, g^{max}_{n,u,t} \qquad \forall n,u, \text{ and } \forall t \geq 2 \tag{8}$$

$$c^{m}_{n,u} - s_{n,u} - M_1(1 - f_{n,u,t}) \leq c^{m}_{k,o} - s_{k,o} + M_1 f_{k,o,t} \qquad \forall t, (n,u) \neq (k,o) \tag{9}$$

$$c^{m}_{n,u} - s_{n,u} - M_1(1 - r_{n,u,t}) \leq c^{m}_{k,o} - s_{k,o} + M_1 f_{k,o,t} \qquad \forall t, (n,u) \neq (k,o) \tag{10}$$

$$
\begin{cases}
\underset{\Omega^{LL}}{\text{Minimize}} \sum_t \sum_n \sum_u \left(c^{up}_{n,u} g^{up}_{n,u,t} - c^{down}_{n,u} g^{down}_{n,u,t} \right) & & & (11) \\
\text{s.t.} & & & \\
cons_{n,t} - \sum_u \left(g^{da}_{n,u,t} + g^{up}_{n,u,t} - g^{down}_{n,u,t} \right) - \sum_k B_{n,k} \delta_{k,t} = 0 & \lambda^{cm}_{n,t} \text{ (free)} & \forall n,t & (12) \\
g^{da}_{n,u,t} + g^{up}_{n,u,t} \leq g^{max}_{n,u,t} & \beta^{up}_{n,u,t} \geq 0 & \forall n,u,t & (13) \\
g^{down}_{n,u,t} \leq g^{da}_{n,u,t} & \beta^{down}_{n,u,t} \geq 0 & \forall n,u,t & (14) \\
g^{up}_{n,u,t} \leq \varepsilon^{reserve^{up}}_{n,u} g^{max}_{n,u,t} & \theta^{up}_{n,u,t} \geq 0 & \forall n,u,t & (15) \\
g^{down}_{n,u,t} \leq \varepsilon^{reserve^{down}}_{n,u} g^{max}_{n,u,t} & \theta^{down}_{n,u,t} \geq 0 & \forall n,u,t & (16) \\
\sum_n H_{\ell,n} \delta_{n,t} \leq cap^{max}_{\ell} & \overline{\mu_{\ell,t}} \geq 0 & \forall \ell,t & (17) \\
-\sum_n H_{\ell,n} \delta_{n,t} \leq cap^{max}_{\ell} & \underline{\mu_{\ell,t}} \geq 0 & \forall \ell,t & (18) \\
sw_n \delta_{n,t} = 0 & \gamma_{n,t} \text{ (free)} & \forall n,t & (19)
\end{cases}
$$

where $\Omega^{UL} = \Big\{ \underbrace{s_{n,u}, g^{da}_{n,u,t}, g^{f}_{n,u,t}, g^{r}_{n,u,t}}_{\geq 0}, \underbrace{f_{n,u,t}, r_{n,u,t}}_{\in\{0,1\}} \Big\}$ and $\Omega^{LL} = \Big\{ \underbrace{g^{up}_{n,u,t}, g^{down}_{n,u,t}}_{\geq 0}, \delta_{n,t} \Big\}$.

The support payments are determined by constraints (9) and (10). If plant (n,u) is fully dispatched and plant (k,o) is not, then the *final* bid price of plant (n,u), i.e., the *original* bid price of (n,u) minus the possible support payment, is less than or equal to the *final* bid price of plant (k,o); otherwise Eq. (9) is not binding. Moreover, constraint (10) requires that the *final* bid price of (n,u) is less than or equal to the *final* bid price of (k,o) if plant (n,u) is partially dispatched and plant (k,o) is not fully dispatched; otherwise, (10) is not binding. Consequently, Eqs. (3)-(10) make sure that no expensive generator is dispatched before the cheaper ones.

At the lower level, the TSO chooses the cost-minimizing (11) deployment of up- ($g^{up}_{n,u,t}$) and down-reserves ($g^{down}_{n,u,t}$) as well as voltage angles ($\delta_{n,t}$) to match supply to demand at every node (12). These nodes represent subregions, which aggregate demand and generation, and in which transmission constraints can be ignored. Eqs. (13)-(16) define the feasible up- and down-reserve deployment intervals for each plant. Furthermore, Eqs. (17)-(19) implement the linearized DC load flow transmission in keeping with Gabriel and Leuthold (2010) and Kunz (2013).

The regulator can perfectly anticipate the outcomes of the lower level. Also, generation cost parameters are not affected by support payments, although producers who do not receive them may increase their bid prices because they know that producers who receive them are dispatched in any case. Consequently, the results of our model on given support payments and the associated costs need to be regarded as a lower bound. This interpretation is supported by the simplification that there is one cost-minimizing TSO inside a price area (in Germany, there are four) and imperfect coordination does not cause extra costs.

In general, bi-level problems of this form require re-formulation as mathematical programs with equilibrium constraints (MPECs) and subsequently as MILPs in order to be solved. However, in this case, our problem has a special structure that reduces it to a single-level problem in which there is no lower-level objective function. This is because all of the terms from the lower-level objective function are present in the upper level and there is no interaction between lower-level dual variables and upper-level primal variables. Thus, the two objective functions are not in conflict, and the upper-level objective function may simply be minimized subject to upper- and lower-level constraints (see Garcés et al. (2009) and Proposition 1 of Zeng and An (2014)). Nevertheless, we will proceed with the re-formulation because a regulator may have other concerns besides simply minimizing generating costs, e.g., minimizing costs of emissions (Siddiqui et al., 2016) or congestion, which may cause the upper- and lower-level objective functions to be in conflict. Indeed, while we use previously developed resolution techniques, our methodological contribution here is the development of a novel set of constraints in Eqs. (3)-(10) that enforce the day-ahead merit order regardless of the objective function. This technique may now be applied by researchers exploring the impact of policy measures on both day-ahead and balancing markets through customized upper-level objective functions. Otherwise, only social welfare maximization would be possible without violating the merit order. We provide the detailed MPEC and MILP formulations in the Appendices A and B, respectively.

4. Numerical examples

4.1. A three-node example

To illustrate the effect of different policies, we run our model with and without support payments as well as a nodal pricing model similar to Kunz (2013) (see Appendix E for the formulation) by considering a three-node network in which there is one generation unit at each node (see Figure 1). The nodes represent locations in the network with generation units and load, while transmission lines connect the nodes. The network as well as demand and generation parameters are in Tables 5 and 6 of the Appendix C, respectively.

The detailed transmission and generation results of our model are in Tables 7 and 8 of Appendix C, while Table 1 summarizes the key outcomes of the policies. In the absence of support payments, only power plants at nodes 1 and 2 are dispatched because they have the lowest bid prices, thereby leading to the lowest day-ahead cost of €3000. However, because lines 2 and 3 to node 3 are congested, the day-ahead solution does not allow demand to be served at node 3. The situation is resolved by deploying down-reserves of the plants at nodes 1 and 2 and up-reserves of the plant at node 3, which causes a re-dispatch cost of €700.

When support payments are introduced, it is optimal to give the plant at node 3 a support payment of €10/MWh. This reduces the bid price of the plant 3 so that it is dispatched in the day-ahead market, thereby replacing part of the generation of the plant at node 2. The support payments increase the cost of day-ahead dispatch to €3600, but now, transmission lines can be utilized to serve demand at all nodes without re-dispatching. Consequently, the total generation cost of €3600 is slightly lower than that of the case without support payments.

Finally, the nodal pricing model achieves an even lower cost of €3300 by considering the transmission constraints already in the day-ahead dispatch. Consequently, the plant at node 3 is dispatched out of merit order in the day-ahead market without giving any support payments.

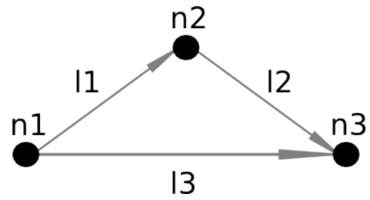

Figure 1: Three-node network indicating conventional direction of flow

measure \ policy	no support	support	nodal
day-ahead cost (€)	3000	3600	3300
re-dispatch cost (€)	700	0	0
total cost (€)	3700	3600	3300
re-dispatch volume (MW)	40	0	0
congested lines	2, 3	1, 3	-

Table 1: Summary of the results of the three-node example

4.2. German power system

Next, we model the German power system to assess the impacts of the different policies on the welfare and power system. More specifically, we use demand, generation and transmission network data from Egerer et al. (2014) to divide Germany into 18 DENA nodes (Deutsche Energie-Agentur, 2010), which correspond to large cities and their surroundings. The nodes and the transmission lines between them are shown in Figure 2. Demand, generation capacity, generation cost, and transmission network parameters are provided in Tables 9-12 of Appendix D, in which we specify the calibration process.

In the following cases, we limit the set of discrete support payment levels only to zero and the differences in bid prices of different power plant types. Other support payment levels would be sub-optimal because the regulator at the upper level can, in view of lower-level outcomes, select which plants to dispatch from a set of plants with equal *final* bid prices. These restrictions decrease the size of the problem and speed up the computation without having an impact on the results. The model is implemented with GAMS 24.2 and solved with CPLEX 12.6 on an Intel i5 2.40GHz processor and 4 GB RAM. The results for the following single- and multi-period cases are computed in less than five seconds. Constraints with continuous variables (such as ramping constraints) are not expected to affect the computational efficiency significantly, whereas new binary variables for constraints (such as startups of power plants) are likely to increase the computation time appreciably.

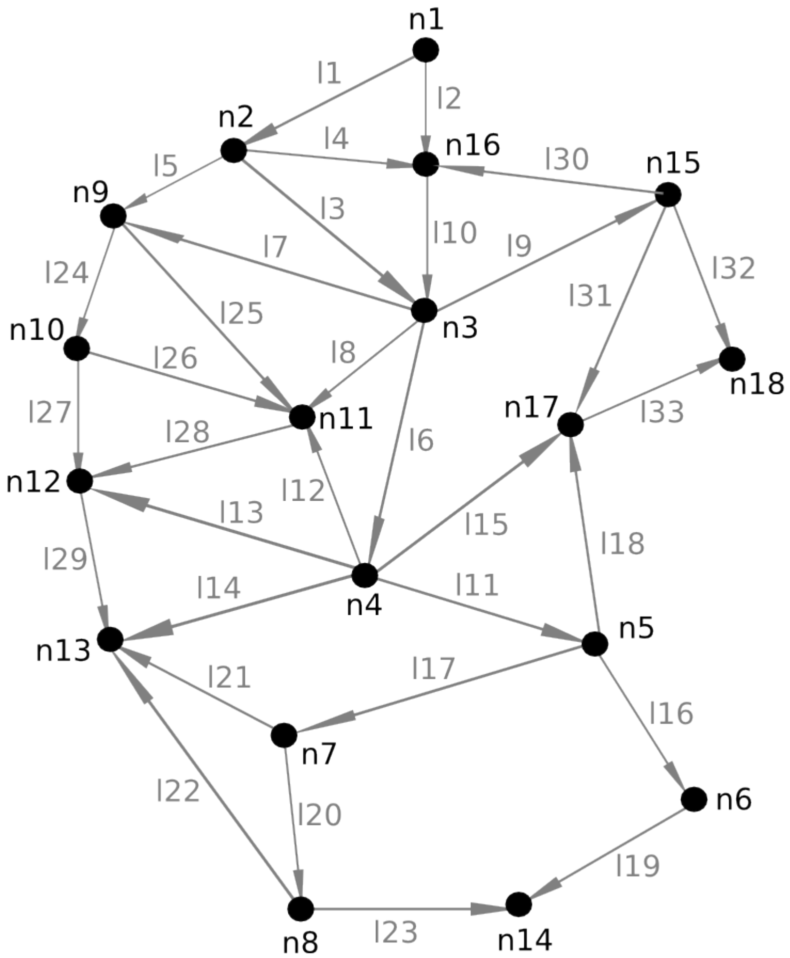

Figure 2: Germany as an 18-node network with 33 cross-node transmission lines

4.3. Single-period case

In the single-period case, we neglect the time index t in the formulation of Section 3. Consequently, constraints (7) and (8) can be disregarded. We examine two scenarios to study the need for support payments. First, in our base scenario, the demand is at the baseline level (Table 9), while wind, solar, and hydro power production are at 40%, 20%, and 20% levels of their maximum generation capacities (Table 10 in Appendix D), respectively. By comparison, since the average wind power generation was 17%, solar 11%, and hydro 13% in 2012 (EEX, 2014), we have taken a day with relatively high renewable generation as our base. In this scenario, support payments do not improve the welfare (see Table 2). Table 13 in Appendix D shows that coal plants are the last plants to be dispatched, and, thus, the day-ahead price is at the level of their bid price of €40/MWh. Only small re-dispatch volumes are needed for (i) some deployment of gas-fired up-reserves in southern and western Germany and (ii) deployment of down-reserves of coal plants in eastern Germany (Table 14 in Appendix D). Table 15 in Appendix D shows that lines l14 and l18 are congested, which indicates strong flow to western and southern Germany.

Second, we run an extreme scenario in which we increase demand by 15% in southern and western German nodes (specifically, nodes 4-14). Furthermore, we increase wind power production to a very high 80% level of maximum capacity and decrease solar power production to 10%, while keeping hydro power production at the 20% level. Such hours occurred, for example, from 3 January 2012 to 5 January 2012, when hourly prices declined to €-75.04/MWh at minimum and increased to €57.42/MWh at maximum. Now, gas plants at nodes 5 (Nuremberg area) and 6 (Munich area) are given an optimal support payment of €15/MWh, which decreases their *final* bid price to the level of coal plants. Consequently, gas plants are dispatched at those nodes, while production from coal plants in northern Germany decreases (Table 16 in Appendix D). Table 17 in Appendix D shows that re-dispatch volumes increase from the base scenario, and up-reserves of gas-fired plants are now deployed in southern and western Germany, whereas the down-reserves of lignite and coal plants are deployed in eastern and northern Germany.

Table 2 shows that support payments increase day-ahead generation costs but decrease re-dispatch costs resulting in equal or lower total costs in both scenarios. In particular, when we disable support payments in the extreme scenario, both re-dispatch volumes and costs triple. The resulting re-dispatch volume of 9.6 GW can be compared with the maximum re-dispatch of 10.8 GW in 2014 (Netztransparenz.de, 2015). However, we note that the change in total welfare is mainly affected by the costs of support payments relative to those of deploying up-reserves, and it is dependent on the parameters $c^{m}_{n,u}$ and $c^{up}_{n,u}$ in the model. Nevertheless, nodal pricing achieves even lower costs in both scenarios. Table 20 in Appendix D shows that nodal pricing finds it optimal to dispatch gas plants in the extreme scenario and that their dispatch at nodes 5 and 6 is close to that of the model with support payments in Table 16 in Appendix D. Consequently, support payments enable policymakers to increase the flexibility and the stability of the power system because they decrease the need for re-dispatch and increase the dispatch of flexible gas-fired plants already in the day-ahead market. Furthermore, the need for north-to-south grid expansion considered by Kunz (2013) is alleviated as nodal pricing and the model with support payments cause the flow to drop in this direction compared to the model without support payments (see Tables 18, 19, and 21 in Appendix D).

Scenario	Base			Extreme		
measure \ policy	no support	support	nodal	no support	support	nodal
day-ahead cost (M€)	1.379	1.379	1.388	1.289	1.400	1.381
re-dispatch cost (M€)	0.018	0.018	0	0.175	0.061	0
total cost (M€)	1.397	1.397	1.388	1.464	1.461	1.381
re-dispatch volume (GW)	1.2	1.2	0	9.6	3.0	0
congested lines	14, 18	14, 18	-	14, 18	14, 18	9, 14, 18

Table 2: Summary of the results of the German single-period case

4.4. Multi-period case

Next, we combine our scenarios in a multi-period model in which the system moves from the base scenario to the extreme scenario. Thus, the main drivers are the increase of wind power from the 40% level to the 80% level, the 15% increase of demand at nodes 4-15, and the decrease of solar power from 20% to 10% level. We note that such a large change is hypothetical, but, given the trend toward increasing penetration of intermittent renewables, greater *absolute* hourly fluctations (in MW) are likely to be observed in the future.

As in the extreme case, we see that a support payment of €15/MWh to gas-fired plants at nodes 5 and 6 displaces coal-fired production in north-eastern Germany (Tables 22 and 23 in Appendix D). Unlike in the single-period base scenario, in which support payments are not optimal, there is now gas-fired production at node 5 at time t1, which decreases the need for re-dispatch by 42% (Table 24 in Appendix D). Consequently, support payments can reduce the costs of re-dispatch under normal, non-extreme wind conditions, too. Similar to the single-period extreme scenario, down-reserves of lignite plants are deployed in eastern Germany in period 2, but, additionally, some slow-ramping coal plants dispatched in period 1 need to deploy their down-reserves in north-eastern Germany.

If we disable support payments in the multi-period case, then there is only a 0.1% increase in total costs (see Table 3), while the re-dispatch volumes increase by 50%. More specifically, the deployment of gas-fired up-reserves and down-reserves of coal as well as lignite plants increases, whereas with support payments, the gas-fired plants offset the significant change in demand and renewable generation already in the day-ahead market. Thus, policymakers can utilize support payments to mitigate short-term variability, which allows for higher penetration of renewables. As a comparison, Table 3 shows that nodal pricing saves 3% on total costs vis-à-vis support payments by eliminating the need for re-dispatching.

policy / measure	no support	support	nodal
day-ahead cost (M€)	2.668	2.732	2.774
re-dispatch cost (M€)	0.193	0.125	0
total cost (M€)	2.861	2.857	2.774
re-dispatch volume (GW)	10.8	7.2	0
congested lines	14, 18	14, 18	9, 14, 18

Table 3: Summary of the results of the German multi-period case

4.5. Sensitivity analysis with respect to uncertainty in demand and renewable generation

To test the robustness of the support payment decisions, we run a stochastic version of the lower-level problem in Eqs. (11)-(19) with fixed upper-level decisions from the single-period extreme scenario in Section 4. Specifically, we introduce imbalances such as demand as well as wind and solar power forecast errors by adding the term $imb_{n,t}$ to the left-hand-side of the nodal power balance equations (12) and evaluate the expected balancing volume and cost by averaging the total balancing volume and cost of all imbalance scenarios, respectively. These scenarios are generated by sampling N unique four-dimensional vectors from quarter-hourly imbalances for the four German TSOs in 2012 (Regelleistung, 2015) using the MATLAB 2015a function *datasample*. Each TSO-wise imbalance is distributed to its nodes in accordance to their shares of demand and generation capacity. The samples have weak positive correlation, and the marginal distributions are characterized by a spike close to zero and relatively fat tails.

With $N = 10000$ and expected imbalances of 1.2 GW, the expected total generation costs with and without support payments are equal at €1.461 million (see Table 4 in which expected congestion is defined as congestion in more than 50% of the scenarios). As the expected balancing volumes are 3.4 GW and 9.7 GW, respectively, both models need to do substantial re-dispatching in order to eliminate the imbalances. By contrast, the nodal pricing model is able to net positive and negative imbalances as the expected re-dispatch volume at 0.8 GW is lower than the expected imbalance. Nevertheless, support payments to gas-fired plants in southern Germany can reduce re-dispatch volumes caused by imbalances substantially, and, thus, respond better to forecast errors of variable renewable generation, for example. Performing the sensitivity analysis with $N = 10000$ scenarios takes approximately seven minutes.

In addition, we test the multi-period model by increasing consumption in the second time step. Only a 3% increase in consumption causes the model without support payments to become infeasible due to inadequate flexibility to deploy down-reserves in northern and eastern Germany and to deploy up-reserves in southern and western Germany. However, the model with support payments finds a solution even when consumption is 9% higher by dispatching gas-fired plants, thereby indicating that policymakers can proactively increase the reliability of the power system with support payments.

measure \ policy	no support	support	nodal
day-ahead cost (M€)	1.289	1.400	1.381
expected re-dispatch cost (M€)	0.172	0.061	0.002
expected total cost (M€)	1.461	1.461	1.383
expected re-dispatch volume (GW)	9.7	3.4	0.8
expected congested lines	14, 18	14, 18	9, 14, 18

Table 4: Summary of the results of the sensitivity analysis

5. Conclusions

In this paper, we have developed a complementarity model to study the impacts of support payments on total generation costs and balancing market volumes in Germany and, thus, their implications for power system flexibility. In our base scenario - which corresponds to normal conditions with modest renewable energy generation - support payments are not needed, but with high wind power production in northern Germany and high demand in southern and western Germany, support payments to gas-fired power plants in southern Germany become optimal.

However, the savings in total generation costs are small because the costs of support payments and re-dispatch largely offset each other, but re-dispatch volumes decrease significantly by a factor of 1 to 2. Moreover, in the multi-period scenario, we find that support payments allow gas-fired plants to be dispatched day-ahead and reduce re-dispatch volumes by offsetting the variability of renewable energy generation by utilizing their fast-ramping capabilities. Even in non-extreme wind conditions, re-dispatch costs are reduced so that the uneven distribution of wind power is mitigated.

Sensitivity analysis of the optimal support payments indicates that they can reduce expected balancing volumes and costs. Also, the power system with support payments is able to withstand quicker changes in consumption and renewable generation. On the other hand, our results show that nodal pricing would be the most effective method to decrease balancing and re-dispatch volumes. However, the regulator has outlined that uniform pricing will be maintained (Bundesministerium für Wirtschaft und Energie (BMWi), 2015). Therefore, support payments would be an effective medium-term measure to integrate renewables. One drawback is that the regulator cannot predict the market outcomes perfectly, and, thus, excess support payments may be needed, thereby resulting in welfare losses. Also, some capacity mechanisms have failed to enforce timely availability (Batlle and Rodilla, 2010).

From the modeling perspective, the lack of cross-border flows and the simplicity of the day-ahead bidding model, in particular, can give overly strong indications about the need for support payments. Extending the model to a stochastic bi-level problem would give more insight into optimal support payments under spatio-temporally correlated imbalances. More extensive vulnerability assessment of short-term supply adequacy could be conducted with a so-called interdiction model, where the upper- and lower-level conflict. On the one hand, future research could seek to develop more detailed short-term models, but on the other hand, long-term security of supply or possible market power issues were not addressed. However, as we maintain the merit order using constraints, we can specify customized objective functions that do not minimize generation costs only, which allows for new types of power market simulations. For example, one such possibility is to replace support payments with CO_2 prices in order to study their impacts on power systems.

Acknowledgements

This research has been supported by funding from the STEEM project of the Aalto Energy Efficiency programme. Siddiqui acknowledges the support of the RISKY-RES project (number 228811) funded by the Research Council of Norway. We are grateful for feedback from attendees of the 2014 GOR, 2015 NESS, and 2015 ISMP conferences. In particular, insights from lead discussant Juan Miguel Morales of DTU at the NESS conference are greatly appreciated. Comments from three anonymous referees and the handling editor have also improved this work. All remaining errors are the authors' own.

References

Baringo, L. and Conejo, A. (2011). Wind power investment within a market environment. *Applied Energy*, 88:3239–3247.

Batlle, C. and Rodilla, P. (2010). A critical assessment of the different approaches aimed to secure electricity generation supply. *Energy Policy*, 38:7169–7179.

Batlle, C., Vázquez, C., Rivier, M., and Pérez-Arriaga, I. J. (2007). Enhancing power supply adequacy in Spain: Migrating from capacity payments to reliability options. *Energy Policy*, 35(9):4545–4554.

Benini, M., Cremonesi, F., Gallanti, M., Gelmini, A., and Martini, R. (2006). Capacity payment schemes in the Italian electricity market. CIGRE General Session.

Bundesministerium für Wirtschaft und Energie (BMWi) (2015). Ein Strommarkt für die Energiewende. Ergebnispapier des Bundesministeriums für Wirtschaft und Energie (Weißbuch).

Caldecott, B. and McDaniels J. (2014). Stranded generation assets: Implications for European capacity mechanisms, energy markets and climate policy. Working paper, Smith School of Enterprise and the Environment, University of Oxford.

Deutsche Energie-Agentur (2010). dena-Netzstudie II. Integration erneuerbarer Energien in die deutsche Stromversorgung im Zeitraum 2015 – 2020 mit Ausblick 2025.

Dupont, B., Jonghe, C. D., Olmos, L., and Belmans, R. (2014). Demand response with locational dynamic pricing to support the integration of renewables. *Energy Policy*, 67:344–354.

EEX (2014). EEX Transparency Platform. `http://www.transparency.eex.com/en/`.

Egerer, J., Gerbaulet, C., Ihlenburg, R., Kunz, F., Reinhard, B., von Hirschhausen, C., Weber, A., and Weibezahn, J. (2014). Electricity sector data for policy-relevant modeling: Data documentation and applications to the German and European electricity markets. *Deutsches Institut für Wirtschaftsforschung*.

Fusco, F., Nolan, G., and Ringwood, J. V. (2010). Variability reduction through optimal combination of wind/wave resources – an Irish case study. *Energy*, 35:314–325.

Gabriel, S. A., Conejo, A. J., Fuller, J. D., Hobbs, B. F., and Ruiz, C. (2013). *Complementarity Modeling in Energy Markets*. Springer, New York.

Gabriel, S. A. and Leuthold, F. U. (2010). Solving discretely-constrained MPEC problems with applications in electric power markets. *Energy Economics*, 32(1):3–14.

Garcés, L. P., Conejo, A. J., García-Bertrand, R., and Romero, R. (2009). A bilevel approach to transmission expansion planning within a market environment. *IEEE Transactions on Power Systems*, 24(3):1513–1522.

German Federal Ministry for Economic Affairs and Energy (BMWi) (2014). An electricity market for Germany's energy transition. Discussion paper of the Federal Ministry for Economic Affairs and Energy (Green paper).

Gutiérrez-Martín, F., Da Silva-Álvarez, R.A., and Montoro-Pintado, P. (2013). Effects of wind intermittency on reduction of CO_2 emissions: The case of the Spanish power system *Energy*, 61:108–117.

Hach, D. and Spinler, S. (2016). Capacity payment impact on gas-fired generation investments under rising renewable feed-in — A real options analysis. *Energy Economics*, 53:270–280.

Hary, N., Rious, V., and Saguan, M. (2016). The electricity generation adequacy problem: Assessing dynamic effects of capacity remuneration mechanisms. *Energy Policy*, 91:113–127.

Huber, M., Dimkova, D., and Hamacher, T. (2014). Integration of wind and solar power in Europe: Assessment of flexibility requirements. *Energy*, 69:236–246.

Jaehnert, S., Wolfgang, O., Farahmand, H., Völler, S., and Huertas-Hernando, D. (2013). Transmission expansion planning in Northern Europe in 2030 — methodology and analyses. *Energy Policy*, 61:125–139.

Jentsch, M., Trost, T., and Sterner, M. (2014). Optimal use of power-to-gas energy storage systems in an 85% renewable energy scenario. *Energy Procedia*, 46:254–261.

Khazaei, J., Downward, A., and Zakeri, G. (2014). Modelling counter-intuitive effects on cost and air pollution from intermittent generation. *Annals of Operations Research*, 222(1):389–418.

Kunz, F. (2013). Improving congestion management: How to facilitate the integration of renewable generation in Germany. *The Energy Journal*, 34(4):55–78.

Leuthold, F. U., Weigt, H., and von Hirschhausen, C. (2008). Efficient pricing for European electricity networks - the theory of nodal pricing applied to feeding-in wind in Germany. *Utilities Policy*, 16(4):284–291.

Leuthold, F. U., Weigt, H., and von Hirschhausen, C. (2012). A large-scale spatial optimization model of the European electricity market. *Networks and Spatial Economics*, 12(1):75–107.

Morales, J. M., Zugno, M., Pineda, S., and Pinson, P. (2014). Electricity market clearing with improved scheduling of stochastic production. *European Journal of Operational Research*, 235(3):765–774.

Netztransparenz.de (2015). Redispatch-Massnahmen. `http://www.netztransparenz.de/de/Redispatch.htm`.

Regelleistung (2015). Platform for control reserve tendering. `https://www.regelleistung.net/ip/action/index`.

Rintamäki, T., Siddiqui, A. S., and Salo, A. (2014). Does renewable energy generation decrease the volatility of electricity prices? A comparative analysis of Denmark and Germany. Working paper, Systems Analysis Laboratory, Aalto University.

Ruiz, C., Conejo, A. J., Fuller, J. D., Gabriel, S. A., and Hobbs, B. F. (2013). A tutorial review of complementarity models for decision-making in energy markets. *EURO Journal on Decision Processes*, 2(1-2):91–120.

Schill, W.-P. and Kemfert, C. (2011). Modeling strategic electricity storage: The case of pumped hydro storage in Germany. *The Energy Journal*, 32(3):59–88.

Siddiqui, A. S., Tanaka, M., and Chen, Y. (2016). Are targets for renewable portfolio standards too low? The impact of market structure on energy policy. *European Journal of Operational Research*, 250(1):328–341.

TenneT TSO GmbH (2013). TenneT reserviert Irsching 4 und 5 für re-dispatch. `http://www.tennet.eu/de/news-presse/article/tennet-reserviert-irsching-4-und-5-fuer-re-dispatch.html`.

Ueckerdt, F., Brecha, R., Luderer G., Sullivan P., Schmid E., Bauer N., Böttger D., and Pietzcker R. (2015). Representing power sector variability and the integration of variable renewables in long-term energy-economy models using residual load duration curves *Energy*, 90:1799–1814.

Van den Bergh, K., Couckuyt, D., Delarue, E., and D'haeseleer, W. (2015). Redispatching in an interconnected electricity system with high renewables penetration. *Electric Power Systems Research*, 127:64–72.

Vazquez, C., Rivier, M., and Perez-Arriaga, I. (2002). A market approach to long-term security of supply. *IEEE Transactions on Power Systems*, 17(2):349–357.

Weigt, H., Jeske, T., Leuthold, F., and von Hirschhausen, C. (2010). Take the long way down: Integration of large-scale North Sea wind using HVDC transmission. *Energy Policy*, 38:3164–3173.

Winkler, J., Gaio, A., Pfluger, B., and Ragwitz, M. (2016). Impact of renewables on electricity markets - Do support schemes matter? *Energy Policy*, 93:157–167.

Würzburg, K., Labandeira, X., and Linares, P. (2013). Renewable generation and electricity prices: Taking stock and new evidence for Germany and Austria. *Energy Economics*, 40 S1:159–171.

Zeng, B. and An, Y. (2014). Solving bilevel mixed integer program by reformulations and decomposition. Working paper, Department of Industrial and Management Systems Engineering, University of South Florida.

Appendix A MPEC formulation

We cast the bi-level program (1)-(19) as a single-level MPEC, which is then used to formulate the linearized model. In the MPEC, the upper-level Eqs. (1)-(10) remain unchanged, and the decision variables consist of upper- and lower-level decision variables as well as the dual variables of the lower-level problem (Gabriel et al., 2013). Since the lower-level problem is convex, it can be replaced by its Karush-Kuhn-Tucker (KKT) conditions (A-2)-(A-12).

$$\underset{\Omega^{UL}\cup\Omega^{LL}\cup\Omega^{DV}}{\text{Minimize}} \sum_t \sum_n \sum_u \left(\left(c^m_{n,u} + s_{n,u}\right) g^{da}_{n,u,t} + c^{up}_{n,u} g^{up}_{n,u,t} - c^{down}_{n,u} g^{down}_{n,u,t} \right) \tag{A-1}$$

s.t.

Eqs. (2)-(10)

$$\lambda^{cm}_{n,t} \text{ (free)}, \; cons_{n,t} - \sum_u (g^{da}_{n,u,t} + g^{up}_{n,u,t} - g^{down}_{n,u,t}) - \sum_k B_{n,k}\delta_{k,t} = 0 \qquad \forall n,t \tag{A-2}$$

$$\delta_{n,t} \text{ (free)}, \; -\sum_k B_{k,n}\lambda^{cm}_{k,t} + \sum_l H_{l,n}\overline{\mu_{l,t}} - \sum_l H_{l,n}\underline{\mu_{l,t}} + sw_n\gamma_{n,t} = 0 \qquad \forall n,t \qquad \text{(A-3)}$$

$$\gamma_{n,t} \text{ (free)}, \; sw_n\delta_{n,t} = 0 \qquad \forall n,t \qquad \text{(A-4)}$$

$$g^{up}_{n,u,t} \geq 0 \perp c^{up}_{n,u} - \lambda^{cm}_{n,t} + \beta^{up}_{n,u,t} + \theta^{up}_{n,u,t} \geq 0 \qquad \forall n,u,t \qquad \text{(A-5)}$$

$$g^{down}_{n,u,t} \geq 0 \perp -c^{down}_{n,u} + \lambda^{cm}_{n,t} + \beta^{down}_{n,u,t} + \theta^{down}_{n,u,t} \geq 0 \qquad \forall n,u,t \qquad \text{(A-6)}$$

$$\beta^{up}_{n,u,t} \geq 0 \perp g^{max}_{n,u,t} - g^{da}_{n,u,t} - g^{up}_{n,u,t} \geq 0 \qquad \forall n,u,t \qquad \text{(A-7)}$$

$$\beta^{down}_{n,u,t} \geq 0 \perp g^{da}_{n,u,t} - g^{down}_{n,u,t} \geq 0 \qquad \forall n,u,t \qquad \text{(A-8)}$$

$$\theta^{up}_{n,u,t} \geq 0 \perp \varepsilon^{reserve^{up}}_{n,u} g^{max}_{n,u,t} - g^{up}_{n,u,t} \geq 0 \qquad \forall n,u,t \qquad \text{(A-9)}$$

$$\theta^{down}_{n,u,t} \geq 0 \perp \varepsilon^{reserve^{down}}_{n,u} g^{max}_{n,u,t} - g^{down}_{n,u,t} \geq 0 \qquad \forall n,u,t \qquad \text{(A-10)}$$

$$\overline{\mu_{\ell,t}} \geq 0 \perp cap^{max}_{\ell} - \sum_n H_{\ell,n}\delta_{n,t} \geq 0 \qquad \forall \ell,t \qquad \text{(A-11)}$$

$$\underline{\mu_{\ell,t}} \geq 0 \perp cap^{max}_{\ell} + \sum_n H_{\ell,n}\delta_{n,t} \geq 0 \qquad \forall \ell,t \qquad \text{(A-12)}$$

where $\Omega^{DV} = \Big\{\lambda^{cm}_{n,t}, \gamma_{n,t}, \underbrace{\beta^{up}_{n,u,t}, \beta^{down}_{n,u,t}, \theta^{up}_{n,u,t}, \theta^{down}_{n,u,t}, \overline{\mu_{\ell,t}}, \underline{\mu_{\ell,t}}}_{\geq 0}\Big\}$.

Appendix B MILP formulation

Our MPEC is non-linear due to the bi-linear terms $s_{n,u}g_{n,u,t}$ in Eq. (A-1) and complementarity conditions (A-5)-(A-12). We apply the linearization procedure of Gabriel and Leuthold (2010). First, the complementarity conditions in (A-5)-(A-12) are associated with disjunctive variables $r1,\dots,r8$ and two corresponding disjunctive constraints in the set of Eqs. (A-20)-(A-35). Second, we introduce valid discrete support payment levels $\bar{s}_{n,u,i}$ and binary indicator variables $q_{n,u,i}$ that equal 1 only when the ith discrete support payment level is selected. Moreover, the binary indicator variables $q^{g^{da}}_{n,u,t}$ equal to 1 when $g^{da}_{n,u,t} > 0$ and 0 otherwise. Thus, the bi-linear terms in the objective function can be replaced with the following variable

$$v_{n,u,i,t} = \begin{cases} \bar{s}_{n,u,i}g^{da}_{n,u,t} \text{ if } q_{n,u,i} = q^{g^{da}}_{n,u,t} = 1 \\ 0 \text{ otherwise} \end{cases} \qquad \text{(A-13)}$$

The logic is modeled with constraints (A-15) - (A-19) as follows. If plant (n,u) is running at time period t, then $q^{g^{da}}_{n,u,t}$ is equal to one (Eq. (A-15)). Constraint (A-16) ensures that the variable $q_{n,u,i}$ is equal to 1 when the ith discrete support payment level $\bar{s}_{n,u,i}$ is selected and zero otherwise. Constraint (A-17) ensures that only one payment level is selected for each (n,u). Next, constraint (A-18) allows the binary variable $q^{v}_{n,u,i,t}$ to be one only if both $q^{g^{da}}_{n,u,t}$ and $q_{n,u,i}$ are one. Consequently, if $q^{v}_{n,u,i,t}$ is zero, then constraint (A-19) drives the bi-linear term $v_{n,u,i,t}$ to zero. When $q^{v}_{n,u,i,t}$ becomes one, the lower bound of $v_{n,u,i,t}$ becomes $\bar{s}_{n,u,i}g^{da}_{n,u,t}$, which is the optimal value for $v_{n,u,i,t}$ to minimize the objective function.

$$\underset{\Omega^{UL}\cup\Omega^{LL}\cup\Omega^{DV}\cup\Phi}{\text{Minimize}} \sum_t\sum_n\sum_u \left[\left(c^{m}_{n,u}g^{da}_{n,u,t} + c^{up}_{n,u}g^{up}_{n,u,t} - c^{down}_{n,u}g^{down}_{n,u,t}\right) + \sum_i v_{n,u,i,t}\right] \tag{A-14}$$

s.t.

$$K_{g^{da}}q^{g^{da}}_{n,u,t} - g^{da}_{n,u,t} \geq 0 \qquad \forall n,u,t \tag{A-15}$$

$$s_{n,u} = \sum_i q_{n,u,i}\bar{s}_{n,u,i} \qquad \forall n,u \tag{A-16}$$

$$\sum_i q_{n,u,i} - 1 = 0 \qquad \forall n,u \tag{A-17}$$

$$\begin{cases} q^{v}_{n,u,i,t} \leq q^{g^{da}}_{n,u,t} \quad \forall n,u,i,t \\ q^{v}_{n,u,i,t} \leq q_{n,u,i} \quad \forall n,u,i,t \\ q_{n,u,i} + q^{g^{da}}_{n,u,t} - 1 \leq q^{v}_{n,u,i,t} \quad \forall n,u,i,t \end{cases} \tag{A-18}$$

$$\begin{cases} 0 \leq v_{n,u,i,t} \leq K_v q^{v}_{n,u,i,t} \quad \forall n,u,i,t \\ 0 \leq \bar{s}_{n,u,i}g^{da}_{n,u,t} - v_{n,u,i,t} \leq K_v(1 - q^{v}_{n,u,i,t}) \quad \forall n,u,i,t \end{cases} \tag{A-19}$$

Eqs. (2)-(10)

Eqs. (A-2)-(A-4)

$$K_1 r1_{n,u,t} \geq c^{up}_{n,u} - \lambda^{cm}_{n,t} + \beta^{up}_{n,u,t} + \theta^{up}_{n,u,t} \geq 0 \qquad \forall n,u,t \tag{A-20}$$

$$K_1(1 - r1_{n,u,t}) \geq g^{up}_{n,u,t} \geq 0 \qquad \forall n,u,t \tag{A-21}$$

$$K_2 r2_{n,u,t} \geq -c^{down}_{n,u} + \lambda^{cm}_{n,t} + \beta^{down}_{n,u,t} + \theta^{down}_{n,u,t} \geq 0 \qquad \forall n,u,t \tag{A-22}$$

$$K_2(1 - r2_{n,u,t}) \geq g^{down}_{n,u,t} \geq 0 \qquad \forall n,u,t \tag{A-23}$$

$$K_3 r3_{n,u,t} \geq g^{max}_{n,u,t} - g^{da}_{n,u,t} - g^{up}_{n,u,t} \geq 0 \qquad \forall n,u,t \tag{A-24}$$

$$K_3(1 - r3_{n,u,t}) \geq \beta^{up}_{n,u} \geq 0 \qquad \forall n,u,t \tag{A-25}$$

$$K_4 r4_{n,u,t} \geq g^{da}_{n,u,t} - g^{down}_{n,u,t} \geq 0 \qquad \forall n,u,t \qquad \text{(A-26)}$$

$$K_4(1 - r4_{n,u,t}) \geq \beta^{down}_{n,u,t} \geq 0 \qquad \forall n,u,t \qquad \text{(A-27)}$$

$$K_5 r5_{n,u,t} \geq \varepsilon^{reserve^{up}}_{n,u} g^{max}_{n,u,t} - g^{up}_{n,u,t} \geq 0 \qquad \forall n,u,t \qquad \text{(A-28)}$$

$$K_5(1 - r5_{n,u,t}) \geq \theta^{up}_{n,u,t} \geq 0 \qquad \forall n,u,t \qquad \text{(A-29)}$$

$$K_6 r6_{n,u,t} \geq \varepsilon^{reserve^{down}}_{n,u} g^{max}_{n,u,t} - g^{down}_{n,u,t} \geq 0 \qquad \forall n,u,t \qquad \text{(A-30)}$$

$$K_6(1 - r6_{n,u,t}) \geq \theta^{down}_{n,u,t} \geq 0 \qquad \forall n,u,t \qquad \text{(A-31)}$$

$$K_7 r7_{\ell,t} \geq cap^{max}_{\ell} - \sum_n H_{\ell,n}\delta_{n,t} \geq 0 \qquad \forall \ell,t \qquad \text{(A-32)}$$

$$K_7(1 - r7_{\ell,t}) \geq \overline{\mu_{\ell,t}} \geq 0 \qquad \forall \ell,t \qquad \text{(A-33)}$$

$$K_8 r8_{\ell,t} \geq cap^{max}_{\ell} + \sum_n H_{\ell,n}\delta_{n,t} \geq 0 \qquad \forall \ell,t \qquad \text{(A-34)}$$

$$K_8(1 - r8_{\ell,t}) \geq \underline{\mu_{\ell,t}} \geq 0 \qquad \forall \ell,t \qquad \text{(A-35)}$$

where $\mathbf{\Phi} = \Big\{ \underbrace{v_{n,u,i,t}}_{\geq 0}, \underbrace{q^{g^{da}}_{n,u,t}, q^{v}_{n,u,i,t}, q_{n,u,i}, r1, \ldots, r8}_{\in\{0,1\}} \Big\}$.

Appendix C Calibration and detailed results of the three-node example

Parameter	l1	l2	l3
cap^{max}_{ℓ} (MW)	10	10	10

Table 5: Network parameters of the three-node example

Parameter	node 1	node 2	node 3
$cons_n$ (MW)	40	40	40
$c^{m}_{n,u}$ (€/MWh)	20	30	40
$c^{up}_{n,u}$ (€/MWh)	60	60	60
$c^{down}_{n,u}$ (€/MWh)	20	30	40
$g^{max}_{n,u}$ (MW)	60	60	60

Table 6: Demand and generation parameters of the three-node example

Support payments	Disabled			Enabled		
	l1	l2	l3	l1	l2	l3
flow (MW)	0	10	10	10	0	10

Table 7: Network flow results of the three-node example

Support payments	Disabled			Enabled		
Variable	node 1	node 2	node 3	node 1	node 2	node 3
$s_{n,u}$ (€/MWh)	0	0	0	0	0	10
$g^{da}_{n,u}$ (MW)	60	60	0	60	30	30
$g^{up}_{n,u}$ (MW)	0	0	20	0	0	0
$g^{down}_{n,u}$ (MW)	10	10	0	0	0	0

Table 8: Generation results of the three-node example

Appendix D Calibration and detailed results of the German power system model

We use data for the 18 DENA nodes from Egerer et al. (2014). The baseline demand for each zone in Table 9 is computed by averaging the off-peak and on-peak demand share of each zone. Furthermore, we scale these figures up by 10% to remove the impact of weekends and holidays.

In compiling the maximum generation capacities in Table 10, we neglect power plants that use biomass, waste, or oil because they have relatively small generation capacities. For simplicity, we combine different types of power plants using the same fuel under one category. Furthermore, the capacities of nuclear, lignite, and coal plants have been reduced by 15% to account for maintenance outages. Table 11 shows the different costs and ramping efficiencies of the power plants based on our rough estimations. We note that wind, solar, and nuclear production cannot be up- or down-reserved and that lignite and coal plants ramp-up relatively slowly, whereas gas-fired plants are characterized by flexibility (Gutiérrez-Martín et al., 2013).

The transmission network parameters in Table 12 have been compiled by adding the thermal capacities, resistances, and reactances of all 220 kV and 380 kV circuits for each pair of nodes. In calculating the thermal capacity, we assume that one 220 kV circuit corresponds to thermal capacity of 490 MW and one 380 kV to 1700 MW (Egerer et al., 2014). We assume bi-directional current flow on every line, and if technical characteristics of the line depend on the flow direction, then we take the maximum of every parameter. To account for network security constraints, we limit the thermal capacity of each line to 80% of the maximum capacity.

	n1	n2	n3	n4	n5	n6	n7	n8	n9	n10	n11	n12	n13	n14	n15	n16	n17	n18
$cons_{n,t}$	1.1	3.0	4.4	3.2	3.1	5.2	3.6	5.4	1.2	9.9	3.7	6.5	5.6	1.5	4.8	1.9	2.4	3.4

Table 9: Baseline demand for each node in GW

node \ type	wind	solar	nuclear	hydro	lignite	coal	gas
n1	3.6	1.1	1.2	0	0	0.4	0
n2	4.4	1.5	0	0	0	1.4	0.7
n3	2.9	1	1.2	0.3	0.3	2	0.6
n4	1	1.4	0	0.7	0	0.9	0.5
n5	0.7	3.3	1.1	0.5	0	0	1.3
n6	0.1	4	1.2	1.4	0	0.7	2.4
n7	0.2	1.3	2.3	0.1	0	1.5	0.6
n8	0.4	3.1	0	2.5	0	0.8	0.4
n9	1.1	1	1.1	0	0	0.7	1.8
n10	0.5	1.4	0	0.2	2.2	6.2	2.6
n11	1.3	1.3	0	0.2	0	1.8	2
n12	1.3	1.1	0	0.2	6.6	0	1.5
n13	1.6	1.8	0	0.2	0	3.1	1.9
n14	0.1	2.1	2.2	0.4	0	0	0.1
n15	7.2	2.7	0	0	0.2	1.1	2.2
n16	0.4	0.2	0	0.1	0	0.4	0.1
n17	2.4	1.7	0	1.6	0.9	0	0.8
n18	2.9	2.5	0	1.2	7.6	0	0.7

Table 10: Maximum generation capacity ($g_{n,u,t}^{max}$) for each node in GW

type	$c_{n,u}^{m}$ (€/MWh)	$c_{n,u}^{up}$ (€/MWh)	$c_{n,u}^{down}$ (€/MWh)	$\varepsilon_{n,u}^{da^{up}}$	$\varepsilon_{n,u}^{da^{down}}$	$\varepsilon_{n,u}^{reserve^{up}}$	$\varepsilon_{n,u}^{reserve^{down}}$
$u1$ (wind)	0	999	-999	1	1	0	0
$u2$ (solar)	0	999	-999	1	1	0	0
$u3$ (nuclear)	1	100	-100	0	0	0	0
$u4$ (hydro)	5	30	5	0.5	0.7	0.5	0.7
$u5$ (lignite)	30	40	25	0.3	0.7	0.2	0.6
$u6$ (coal)	40	50	35	0.3	0.7	0.2	0.6
$u7$ (gas)	55	65	55	0.9	1	0.8	0.9

Table 11: Power plant cost and efficiency parameters

line	capacity (GW)	resistance (Ω)	reactance (Ω)
l1	2.7	1.7	14.9
l2	4.3	11.4	67.5
l3	2.2	5.2	38.3
l4	2.7	3.2	27.4
l5	2.7	1.4	7.7
l6	3.5	3.5	27.3
l7	1.4	2.4	20.6
l8	3.5	5	31.7
l9	2.7	1.5	12.7
l10	2.7	0.9	7.4
l11	2.7	4.4	38
l12	4.1	2.6	22.8
l13	1.4	1.6	14.2
l14	2.7	1.3	11.5
l15	2.7	5.7	49
l16	5.3	17.9	115.4
l17	2.7	5.8	50.4
l18	2.7	1.7	14.6
l19	2.7	1.5	13
l20	9.4	15	122.9
l21	2.6	15.4	98.2
l22	2.7	13.3	72
l23	6.6	8.9	56.5
l24	3.1	9.1	66.4
l25	3.1	8.1	61.8
l26	4.3	11.8	66.2
l27	13.4	15.6	102.5
l28	0.8	3.1	16.6
l29	7.6	20.7	147.3
l30	2.7	2.6	22.7
l31	2.7	3.6	31
l32	5.8	20.5	165.4
l33	5.3	33.1	212.7

Table 12: Transmission network parameters

node \ type	wind	solar	nuclear	hydro	lignite	coal	gas
n1	1.44	0.22	1.19			0.43	
n2	1.76	0.30				1.36	
n3	1.16	0.20	1.19	0.06	0.34	2.04	
n4	0.40	0.28		0.14		0.94	
n5	0.28	0.66	1.11	0.10			
n6	0.04	0.80	1.19	0.28		0.68	
n7	0.08	0.26	2.30	0.02		1.53	
n8	0.16	0.62		0.50		0.77	
n9	0.44	0.20	1.11			0.68	
n10	0.20	0.28		0.04	2.21	6.21	
n11	0.52	0.26		0.04		1.79	
n12	0.52	0.22		0.04	6.63		
n13	0.64	0.36		0.04		3.06	
n14	0.04	0.42	2.21	0.08			
n15	2.88	0.54			0.17	0.76	
n16	0.16	0.04		0.02		0.43	
n17	0.96	0.34		0.32	0.85		
n18	1.16	0.50		0.24	7.57		

Table 13: Day-ahead generation of each power plant type in GW in the base scenario (empty cells are zero)

node \ type	coal	gas
n7		0.43
n13		0.17
n15	-0.59	

Table 14: Deployment of up- and down-reserves in the base scenario (empty rows and columns have been removed to save space)

l1 1.67	l2 0.51	l3 0.42	l4 0.45	l5 1.24	l6 -1.93	l7 -0.18	l8 1.25	l9 -1.12	l10 -0.87	l11 -0.07
l12 -0.56	l13 -0.72	l14* 2.70	l15 -0.86	l16 1.33	l17 0.36	l18* -2.70	l19 -0.85	l20 1.19	l21 0.15	l22 -1.79
l23 -0.36	l24 0.78	l25 0.71	l26 -0.12	l27 -0.06	l28 0.14	l29 0.28	l30 0.34	l31 0.81	l32 -3.35	l33 -2.70

Table 15: Transmission flows in the base scenario (congested lines are indicated by *)

	Support payments enabled							Support payments disabled					
node \ type	wind	solar	nuclear	hydro	lignite	coal	gas	wind	solar	nuclear	hydro	lignite	coal
n1	2.88	0.11	1.19					2.88	0.11	1.19			0.26
n2	3.52	0.15						3.52	0.15				0.48
n3	2.32	0.10	1.19	0.06	0.34			2.32	0.10	1.19	0.06	0.34	2.03
n4	0.80	0.14		0.14		0.94		0.80	0.14		0.14		0.94
n5	0.56	0.33	1.11	0.10			1.05	0.56	0.33	1.11	0.10		
n6	0.08	0.40	1.19	0.28		0.68	2.39	0.08	0.40	1.19	0.28		0.68
n7	0.16	0.13	2.30	0.02		1.53		0.16	0.13	2.30	0.02		1.53
n8	0.32	0.31		0.50		0.77		0.32	0.31		0.50		0.77
n9	0.88	0.10	1.11					0.88	0.10	1.11			0.68
n10	0.40	0.14		0.04	2.21	6.21		0.40	0.14		0.04	2.21	6.21
n11	1.04	0.13		0.04		1.79		1.04	0.13		0.04		1.79
n12	1.04	0.11		0.04	6.63			1.04	0.11		0.04	6.63	
n13	1.28	0.18		0.04		3.06		1.28	0.18		0.04		3.06
n14	0.08	0.21	2.21	0.08				0.08	0.21	2.21	0.08		
n15	5.76	0.27			0.17			5.76	0.27			0.17	
n16	0.32	0.02		0.02				0.32	0.02		0.02		
n17	1.92	0.17		0.32	0.85			1.92	0.17		0.32	0.85	
n18	2.32	0.25		0.24	7.57			2.32	0.25		0.24	7.57	

Table 16: Day-ahead generation of each power plant type in GW in the extreme scenario with and without support payments (empty cells are zero)

node \ type	Support payments enabled: lignite	Support payments enabled: gas	Support payments disabled: lignite	Support payments disabled: coal	Support payments disabled: gas
n1				-0.26	
n2				-0.48	
n3				-0.97	
n5		0.22			1.04
n6					1.92
n7		0.48			0.48
n8		0.32			0.32
n13		0.69			0.97
n14					0.08
n17	-0.51		-0.51		
n18	-1.20		-2.60		

Table 17: Deployment of up- and down-reserves in the extreme scenario with and without support payments (empty rows and columns have been removed to save space)

l1 2.40	l2 0.68	l3 0.58	l4 1.09	l5 1.42	l6 2.22	l7 0.36	l8 1.72	l9 -2.57	l10 -1.53	l11 -0.58
l12 -0.25	l13 -0.05	l14* 2.70	l15 -1.25	l16 1.10	l17 0.84	l18* -2.70	l19 0.18	l20 1.17	l21 0.11	l22 -1.82
l23 -0.98	l24 1.37	l25 0.77	l26 -0.65	l27 -0.37	l28 0.29	l29 0.21	l30 0.94	l31 1.03	l32 -3.17	l33 -2.59

Table 18: Transmission flows in the extreme scenario with support payments (congested lines are denoted with *)

l1 2.38	l2 0.70	l3 0.59	l4 0.90	l5 1.60	l6 2.49	l7 0.10	l8 1.82	l9 -1.80	l10 -1.35	l11 -0.25
l12 -0.42	l13 -0.20	l14* 2.70	l15 -1.00	l16 1.26	l17 0.78	l18* -2.70	l19 -0.13	l20 1.21	l21 0.01	l22 -2.02
l23 -0.76	l24 1.46	l25 0.91	l26 -0.61	l27 -0.33	l28 0.40	l29 0.23	l30 0.56	l31 1.36	l32 -2.36	l33 -2.01

Table 19: Transmission flows in the extreme scenario without support payments (congested lines are denoted with *)

node \ type	wind	solar	nuclear	hydro	lignite	coal	gas
n1	2.88	0.11	1.19				
n2	3.52	0.15					
n3	2.32	0.10	1.19	0.06	0.34		
n4	0.80	0.14		0.14		0.94	
n5	0.56	0.33	1.11	0.10			1.30
n6	0.08	0.40	1.19	0.28		0.68	2.31
n7	0.16	0.13	2.30	0.02		1.53	0.55
n8	0.32	0.31		0.50		0.77	0.26
n9	0.88	0.10	1.11				
n10	0.40	0.14		0.04	2.21	6.00	
n11	1.04	0.13		0.04		1.79	
n12	1.04	0.11		0.04	6.63		
n13	1.28	0.18		0.04		3.06	0.73
n14	0.08	0.21	2.21	0.08			
n15	5.76	0.27			0.17		
n16	0.32	0.02		0.02			
n17	1.92	0.17		0.32			
n18	2.32	0.25		0.24	6.91		

Table 20: Day-ahead generation of each power plant type in GW in the extreme scenario with nodal pricing

l1 2.40	l2 0.68	l3 0.58	l4 1.13	l5 1.39	l6 2.27	l7 0.41	l8 1.77	l9* -2.70	l10 -1.56	l11 -0.58
l12 -0.23	l13 -0.02	l14* 2.70	l15 -1.25	l16 1.15	l17 0.82	l18* -2.70	l19 0.15	l20 1.21	l21 0.12	l22 -1.87
l23 -0.96	l24 1.45	l25 0.78	l26 -0.72	l27 -0.42	l28 0.29	l29 0.21	l30 1.00	l31 1.13	l32 -3.47	l33 -2.84

Table 21: Transmission flows in the extreme scenario with nodal pricing

node \ type	wind		solar		nuclear		hydro		lignite		coal		gas	
	t1	t2	t1	t2	t1	t2	t1	t2	t1	t2	t1	t2	t1	t2
n1	1.44	2.88	0.22	0.11	1.19	1.19					0.43	0.26		
n2	1.76	3.52	0.30	0.15							1.36	0.60		
n3	1.16	2.32	0.20	0.10	1.19	1.19	0.06	0.06	0.34	0.34	2.04	0.61		
n4	0.40	0.80	0.28	0.14			0.14	0.14			0.94	0.94		
n5	0.28	0.56	0.66	0.33	1.11	1.11	0.10	0.10					0.26	1.30
n6	0.04	0.08	0.80	0.40	1.19	1.19	0.28	0.28			0.68	0.68		0.34
n7	0.08	0.16	0.26	0.13	2.30	2.30	0.02	0.02			1.53	1.53		
n8	0.16	0.32	0.62	0.31			0.50	0.50			0.77	0.77		
n9	0.44	0.88	0.20	0.10	1.11	1.11					0.68	0.20		
n10	0.20	0.40	0.28	0.14			0.04	0.04	2.21	2.21	6.21	6.21		
n11	0.52	1.04	0.26	0.13			0.04	0.04			1.79	1.79		
n12	0.52	1.04	0.22	0.11			0.04	0.04	6.63	6.63				
n13	0.64	1.28	0.36	0.18			0.04	0.04			3.06	3.06		
n14	0.04	0.08	0.42	0.21	2.21	2.21	0.08	0.08						
n15	2.88	5.76	0.54	0.27					0.17	0.17	0.50			
n16	0.16	0.32	0.04	0.02			0.02	0.02			0.43	0.13		
n17	0.96	1.92	0.34	0.17			0.32	0.32	0.85	0.85				
n18	1.16	2.32	0.50	0.25			0.24	0.24	7.57	7.57				

Table 22: Day-ahead generation in each power plant type in the multi-period case with support payments (empty cells are zero)

type / node	wind		solar		nuclear		hydro		lignite		coal	
	t1	t2	t1	t2	t1	t2	t1	t2	t1	t2	t1	t2
n1	1.44	2.88	0.22	0.11	1.19	1.19					0.43	0.26
n2	1.76	3.52	0.30	0.15							1.36	0.82
n3	1.16	2.32	0.20	0.10	1.19	1.19	0.06	0.06	0.34	0.34	2.04	1.06
n4	0.40	0.80	0.28	0.14			0.14	0.14			0.94	0.94
n5	0.28	0.56	0.66	0.33	1.11	1.11	0.10	0.10				
n6	0.04	0.08	0.80	0.40	1.19	1.19	0.28	0.28			0.68	0.68
n7	0.08	0.16	0.26	0.13	2.30	2.30	0.02	0.02			1.53	1.53
n8	0.16	0.32	0.62	0.31			0.50	0.50			0.77	0.77
n9	0.44	0.88	0.20	0.10	1.11	1.11					0.68	0.68
n10	0.20	0.40	0.28	0.14			0.04	0.04	2.21	2.21	6.21	6.21
n11	0.52	1.04	0.26	0.13			0.04	0.04			1.79	1.79
n12	0.52	1.04	0.22	0.11			0.04	0.04	6.63	6.63		
n13	0.64	1.28	0.36	0.18			0.04	0.04			3.06	3.06
n14	0.04	0.08	0.42	0.21	2.21	2.21	0.08	0.08				
n15	2.88	5.76	0.54	0.27					0.17	0.17	0.76	0.38
n16	0.16	0.32	0.04	0.02			0.02	0.02			0.43	0.26
n17	0.96	1.92	0.34	0.17			0.32	0.32	0.85	0.85		
n18	1.16	2.32	0.50	0.25			0.24	0.24	7.57	7.57		

Table 23: Day-ahead generation in each power plant type in the multi-period case without support payments (empty cells are zero)

node \ type	Support payments enabled						Support payments disabled					
	lignite		coal		gas		lignite		coal		gas	
	t1	t2	t1	t2	t1	t2	t1	t2	t1	t2	t1	t2
n1				-0.26						-0.26		
n2				-0.60						-0.82		
n3				-0.61								1.04
n5											0.42	1.92
n6						1.92						
n7						0.48						0.48
n8						0.32						0.32
n9				-0.20								
n13					0.34	0.71					0.17	0.97
n14						0.08						0.08
n15			-0.34						-0.59	-0.38		
n16				-0.13						-0.26		
n17		-0.51						-0.51				
n18		-1.20						-2.60				

Table 24: Deployment of up- and down-reserves in the multi-period case with and without support payments (empty rows and columns have been removed to save space)

Appendix E Nodal pricing model

For the nodal pricing model below, we introduce non-negative dual variables $\beta^{da^{up}}_{n,u,t}$ and $\beta^{da^{down}}_{n,u,t}$ for Eqs. (A-39) and (A-40), respectively.

$$\underset{\substack{g^{da}_{n,u,t},\delta_{n,u,t} \\ \geq 0}}{\text{Minimize}} \sum_t \sum_n \sum_u c^m_{n,u} g^{da}_{n,u,t} \quad \text{(A-36)}$$

s.t.

$$cons_{n,t} - \sum_u g^{da}_{n,u,t} - \sum_k B_{n,k}\delta_{k,t} = 0 \qquad \lambda^{cm}_{n,t} \text{ (free)} \qquad \forall n,t \quad \text{(A-37)}$$

$$g^{da}_{n,u,t} \leq g^{max}_{n,u,t} \qquad \beta^{up}_{n,u,t} \geq 0 \qquad \forall n,u,t \quad \text{(A-38)}$$

$$g^{da}_{n,u,t} - g^{da}_{n,u,t-1} \leq \varepsilon^{da^{up}}_{n,u} g^{max}_{n,u,t} \qquad \beta^{da^{up}}_{n,u,t} \geq 0 \qquad \forall n,u, \text{ and } \forall t \geq 2 \tag{A-39}$$

$$g^{da}_{n,u,t-1} - g^{da}_{n,u,t} \leq \varepsilon^{da^{down}}_{n,u} g^{max}_{n,u,t} \qquad \beta^{da^{down}}_{n,u,t} \geq 0 \qquad \forall n,u, \text{ and } \forall t \geq 2 \tag{A-40}$$

$$\sum_n H_{\ell,n} \delta_{n,t} \leq cap^{max}_{\ell} \qquad \overline{\mu_{\ell,t}} \geq 0 \qquad \forall \ell, t \tag{A-41}$$

$$-\sum_n H_{\ell,n} \delta_{n,t} \leq cap^{max}_{\ell} \qquad \underline{\mu_{\ell,t}} \geq 0 \qquad \forall \ell, t \tag{A-42}$$

$$sw_n \delta_{n,t} = 0 \qquad \gamma_{n,t} \text{ (free)} \qquad \forall n, t \tag{A-43}$$